

# Using SEVIRI visible reflectances and RTTOV-MFASIS for the evaluation of ICON model clouds

Christina Stumpf, Christina Köpken-Watts, Leonhard Scheck, Florian Baur (DWD, Germany)

As a step towards the assimilation of visible reflectances also in the global ICON, we study the model clouds using fast forward computations with RTTOV-MFASIS and observed visible reflectances from SEVIRI/MSG. The aim is to better understand characteristics of occurring differences and their dependencies as the global model context presents a wider range of cloud types and viewing geometries than the regional model setup where the VIS assimilation will become operational first (March 2023). Therefore, reflectance histograms and OBS-model departures are

investigated as a function of different influencing factors, like model resolution, particle radii assumptions, viewing geometry and cloud types. This may also guide the need and formulation of situation dependent bias corrections and the setting of observation errors for the assimilation. Additionally to the departures, RTTOV-MFASIS is compared to the more accurate, but considerably slower, DISORT implementation (RTTOV-DOM) to understand possible error contributions resulting from the fast forward model approximation.

## MFASIS simulation

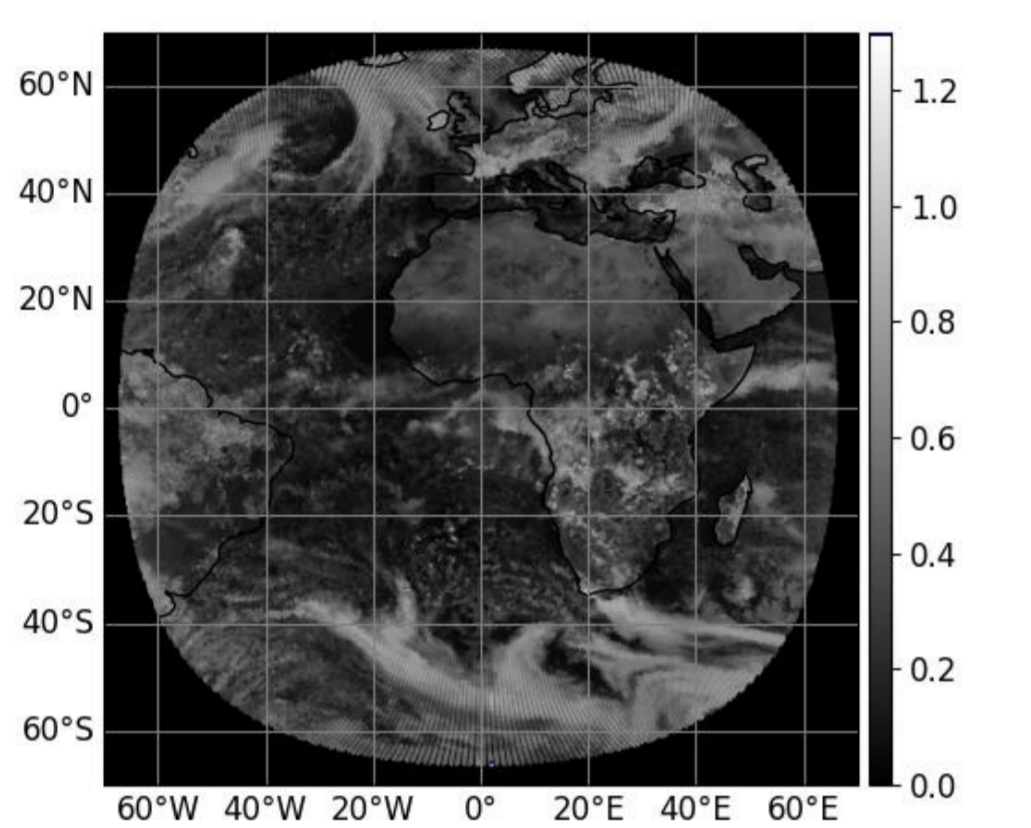


Fig.1: Simulated image @ 0.6  $\mu\text{m}$  using 40 km ICON model fields for 15 March 2021, 12 UTC.

## 1. Forward model and used data

The fast LUT-based forward model MFASIS as implemented in RTTOV v13.1 (Scheck et al., 2016; Saunders et al., 2020) is used in this study for computing cloud affected reflectances based on model profiles from the global ICON model. These are compared to visible reflectances at 0.6  $\mu\text{m}$ , 0.8  $\mu\text{m}$  and 1.6  $\mu\text{m}$  from SEVIRI. The observations are used at original full resolution and averaged onto the ICON model grid. The comparisons shown are based on the two weeks 15-21 Nov and 15-21 March 2021 using daytime imagery at 6, 9, 12, 15, and 18 UTC. Satellite and solar zenith angles are limited to 75° and sunglint is excluded.

## 2. MFASIS compared to RTTOV-DOM

MFASIS has been compared to RTTOV-DOM (using 16 streams) and the differences analysed as a function of various parameters, e.g. the viewing geometry (Fig. 2.) and the presence of water or ice clouds (Fig. 3). Water and ice cloud situations have been selected with thresholds on their respective optical depths in the model profiles. Overall, reflectance differences to RTTOV-DOM are nearly in all situations below 0.05 and there is only marginal dependency on satellite zenith angle or scattering angle (up to about 135°).

## MFASIS compared to RTTOV-DOM

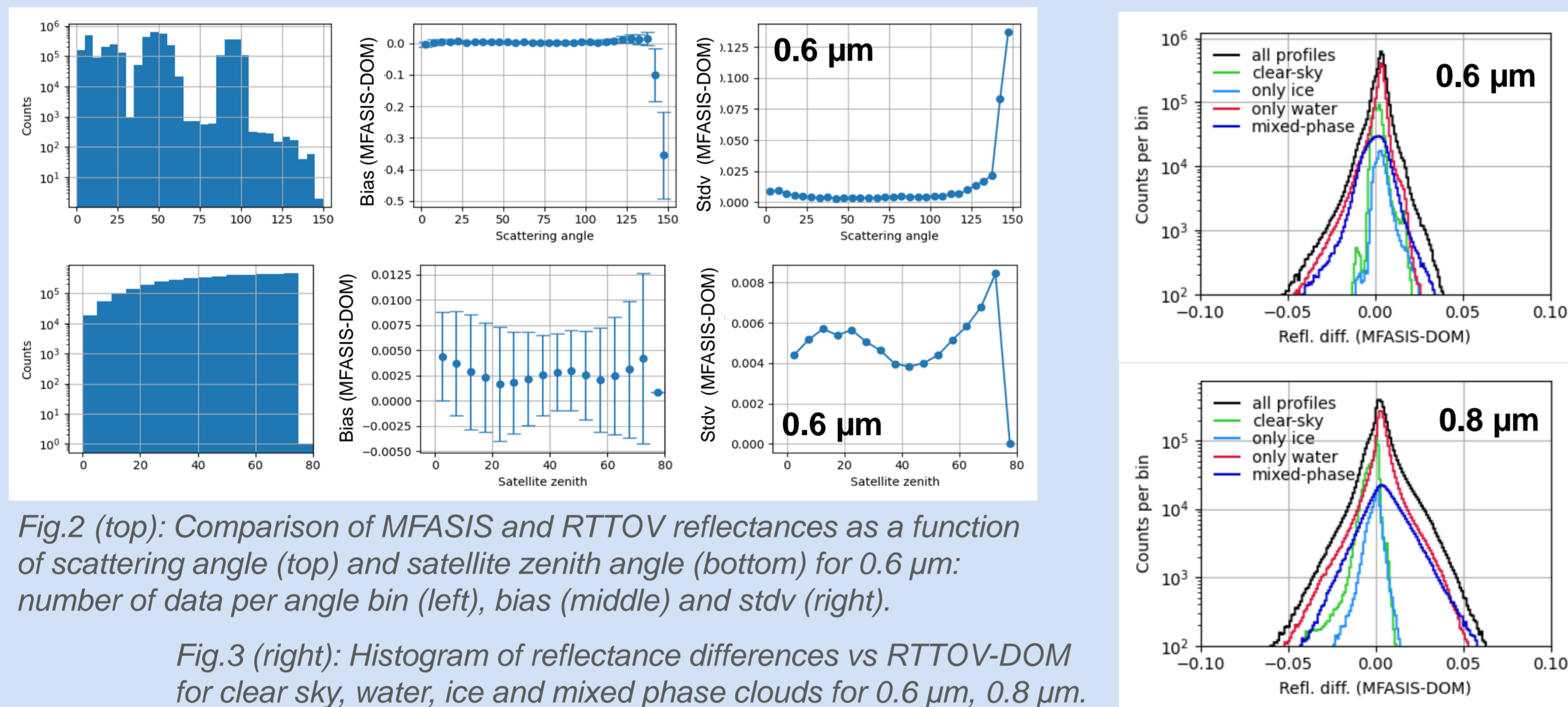


Fig.2 (top): Comparison of MFASIS and RTTOV reflectances as a function of scattering angle (top) and satellite zenith angle (bottom) for 0.6  $\mu\text{m}$ : number of data per angle bin (left), bias (middle) and stdv (right).

Fig.3 (right): Histogram of reflectance differences vs RTTOV-DOM for clear sky, water, ice and mixed phase clouds for 0.6  $\mu\text{m}$ , 0.8  $\mu\text{m}$ .

## 3. Dependency of MFASIS results on cloud particle radii

The real effective radii of cloud water and cloud ice particles are not known and either the RTTOV parameterization or modelled values can be used in RTTOV/MFASIS. Fig. 4 shows the sensitivity of the forward calculations to different particle radii value specifications and results for 1.6  $\mu\text{m}$  have a larger dependency on cloud particle radii than those at 0.6  $\mu\text{m}$  and 0.8  $\mu\text{m}$  (visible for cloudy reflectances above about 0.2). This is consistent with different absorption characteristics at these frequencies. Overall, the difference between observations and forward computations are larger than the variations due to different particle radii assumptions, which is encouraging both in a model cloud evaluation as well as in a reflectance assimilation context.

## Dependency of forward model results on cloud and ice particle radii assumptions

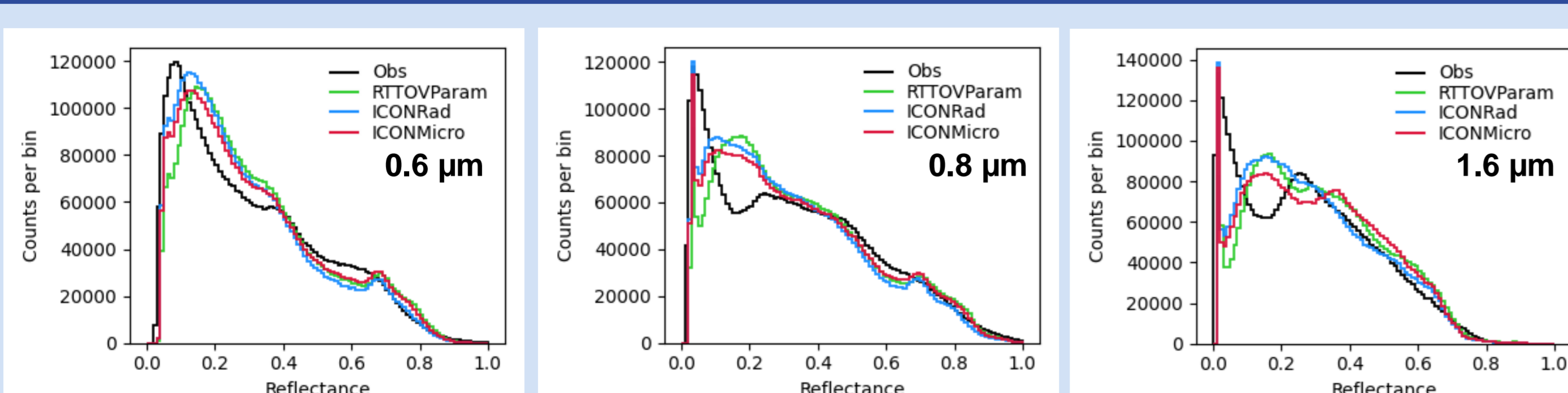


Fig.4: Reflectance histograms for observations at 0.6  $\mu\text{m}$  (left), 0.8  $\mu\text{m}$  (middle), 1.6  $\mu\text{m}$  (right) and corresponding MFASIS simulations based on ICON profiles (40 km model resolution) using particle effective radii of the RTTOV parameterizations (green), the ICON radiation scheme (blue) and radii consistent with ICON microphysics (red).

## 4. Influence of NWP model resolution

As the accuracy of cloud representation in a numerical simulation can depend on model resolution, the comparisons in this study are done for both, the operational deterministic model resolution at 13 km as well as the 40 km resolution of the ICON-EPS system. Fig. 5 compares respective reflectance histograms and shows that the differences due to varying model resolution are mostly small compared to the difference between model and observations which are most pronounced at reflectivities below about 0.4.

## Histograms for ICON at 13 km and 40 km resolution

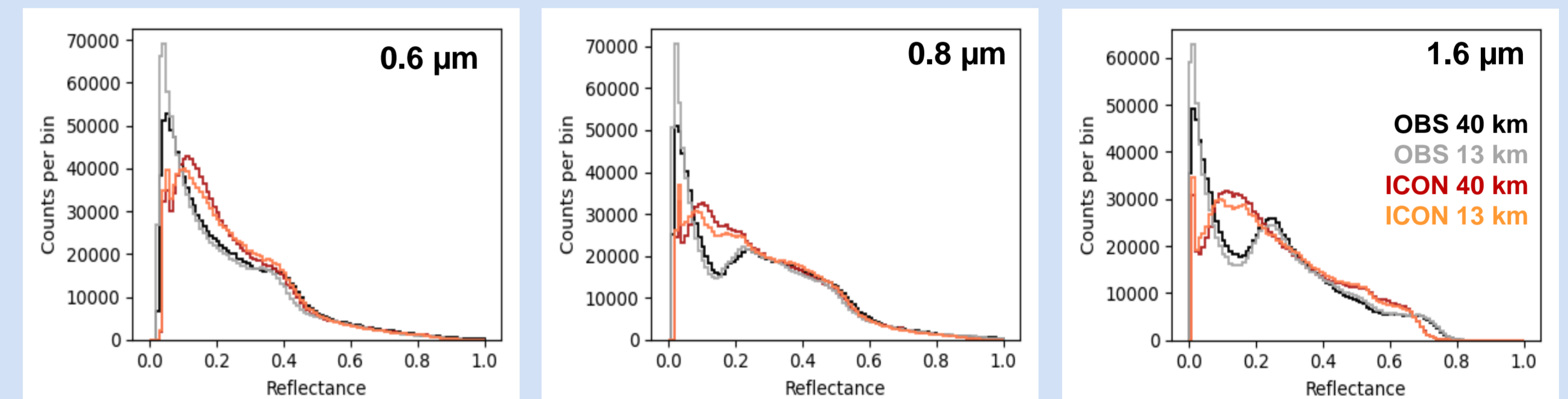


Fig.5: Reflectance histograms for observations at 0.6  $\mu\text{m}$  (left), 0.8  $\mu\text{m}$  (middle), 1.6  $\mu\text{m}$  (right) and corresponding MFASIS simulations based on ICON profiles for comparisons at two different model resolutions: 40 km (the resolution of ensemble system ICON-EPS members) and 13 km (resolution of ICON deterministic system). Data with satellite zenith angles above 50 deg are excluded; here, MFASIS uses particle radii from the ICON radiation scheme.

## 5. OBS minus model statistics

Statistics of reflectance difference between model and observation (Fig. 6) for 0.6  $\mu\text{m}$  show a nearly symmetric behaviour. Results for the 0.8  $\mu\text{m}$  and 1.6  $\mu\text{m}$  channels are broadly similar. For analysing model cloud errors, we have to be aware of other possible error sources like observation and forward model errors. Here, MFASIS errors play a minor role, being at least a magnitude smaller (see Fig. 3) and also the uncertainty in cloud particle radii seems not to be a dominant error source (see Fig. 4). We also stratify the statistics, e.g. for land, sea and different areas. Fig. 6 shows that in the tropics errors are larger, esp. over land, than in mid-latitudes.

For studying different cloud types, we applied a symmetric selection, classifying observations according to the EUMETSAT Optimal Cloud Analysis (OCA) product and model cloud according to cloud water and ice optical thicknesses. Results indicate larger deviations for tropical water clouds (again esp. over land) which could be linked to model cloud water contents or also cloud coverage. A more detailed analysis is ongoing using additionally IR channel observations to add cloud height information.

## Reflectances based on ICON compared to SEVIRI 0.6 micrometers observations

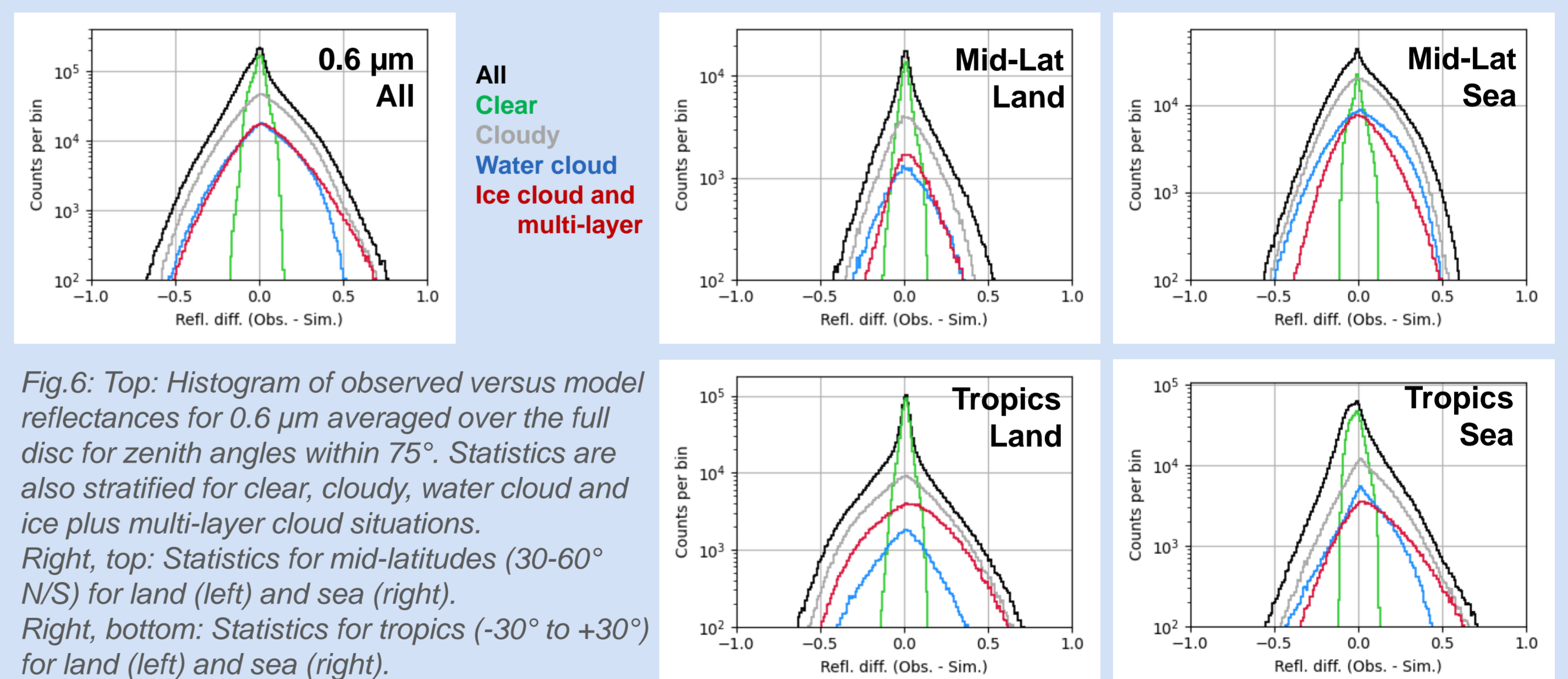


Fig.6: Top: Histogram of observed versus model reflectances for 0.6  $\mu\text{m}$  averaged over the full disc for zenith angles within 75°. Statistics are also stratified for clear, cloudy, water cloud and ice plus multi-layer cloud situations. Right, top: Statistics for mid-latitudes (30-60° N/S) for land (left) and sea (right). Right, bottom: Statistics for tropics (-30° to +30°) for land (left) and sea (right).

## Conclusion and outlook

Using visible reflectances in conjunction with the fast forward operator MFASIS allows new insights into model clouds. This ongoing study will be extended to use the neural network version of MFASIS with the latest improvements for the 1.6  $\mu\text{m}$  channel as implemented in RTTOV v13.2. Also, comparisons of 1-moment and 2-moment physics results (global ICON, ICON-D2 and RUC systems) will be done and observational data use extended to other imagers on geostationary and polar orbiting satellites.

